Supplemental Figures

Figure S1

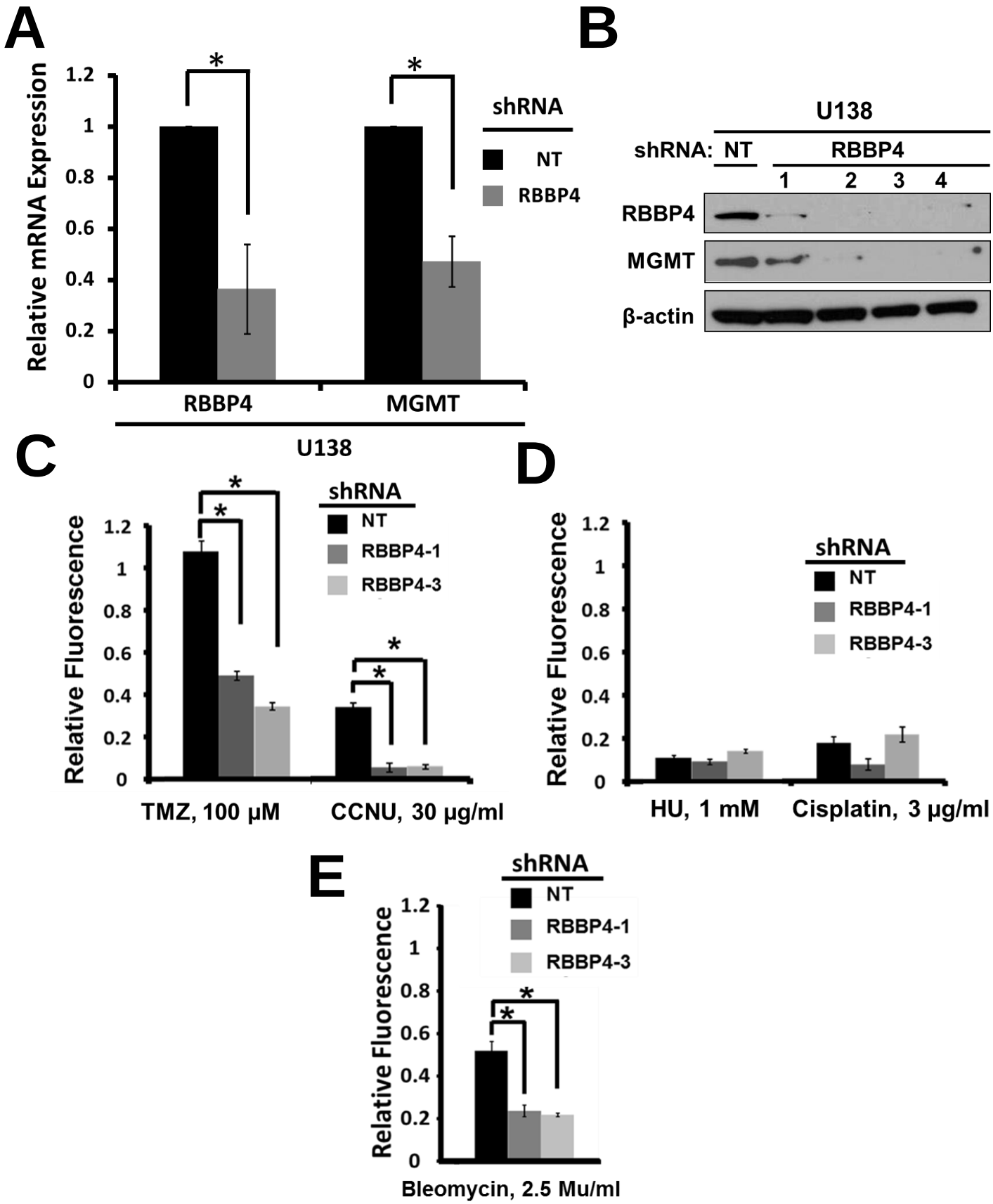

Figure S2

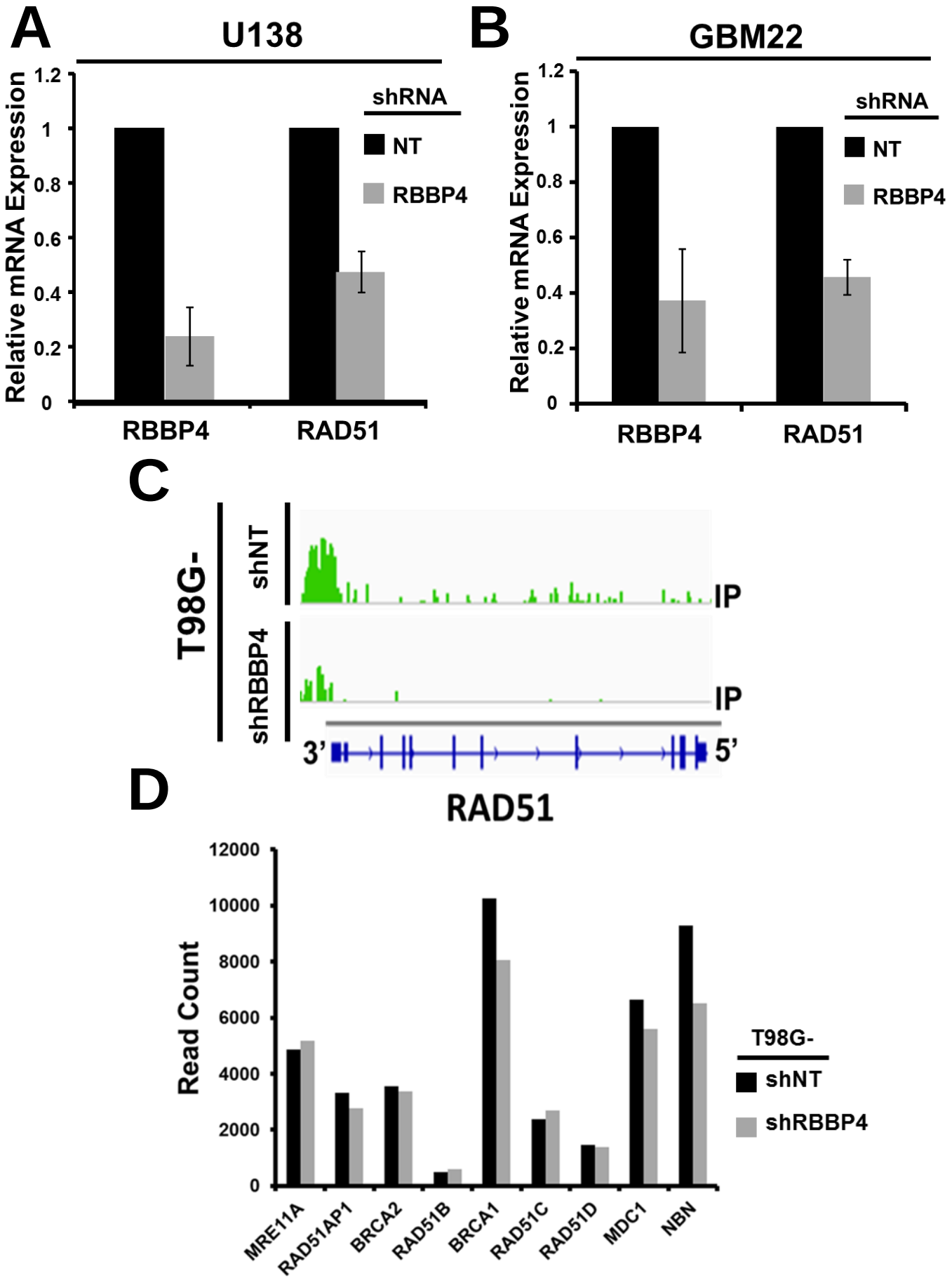
A
U138
Relative mRNA Expression
1.2
1
0.8
0.6
0.4
0.2
0
shRNA
NT
RBBP4
RBBP4
RAD51
B
GBM22
Relative mRNA Expression
1.2
1
0.8
0.6
0.4
0.2
0
shRNA
NT
RBBP4
RBBP4
RAD51
C
T98G-
shNT
IP
shRBBP4
IP
3'
5'
D
RAD51
Read Count
12000
10000
8000
6000
4000
2000
0
MRE11A
RAD51AP1
BRCA2
RAD51B
BRCA1
RAD51C
RAD51D
MDC1
NBN
T98G-
shNT
shRBBP4

Figure S3

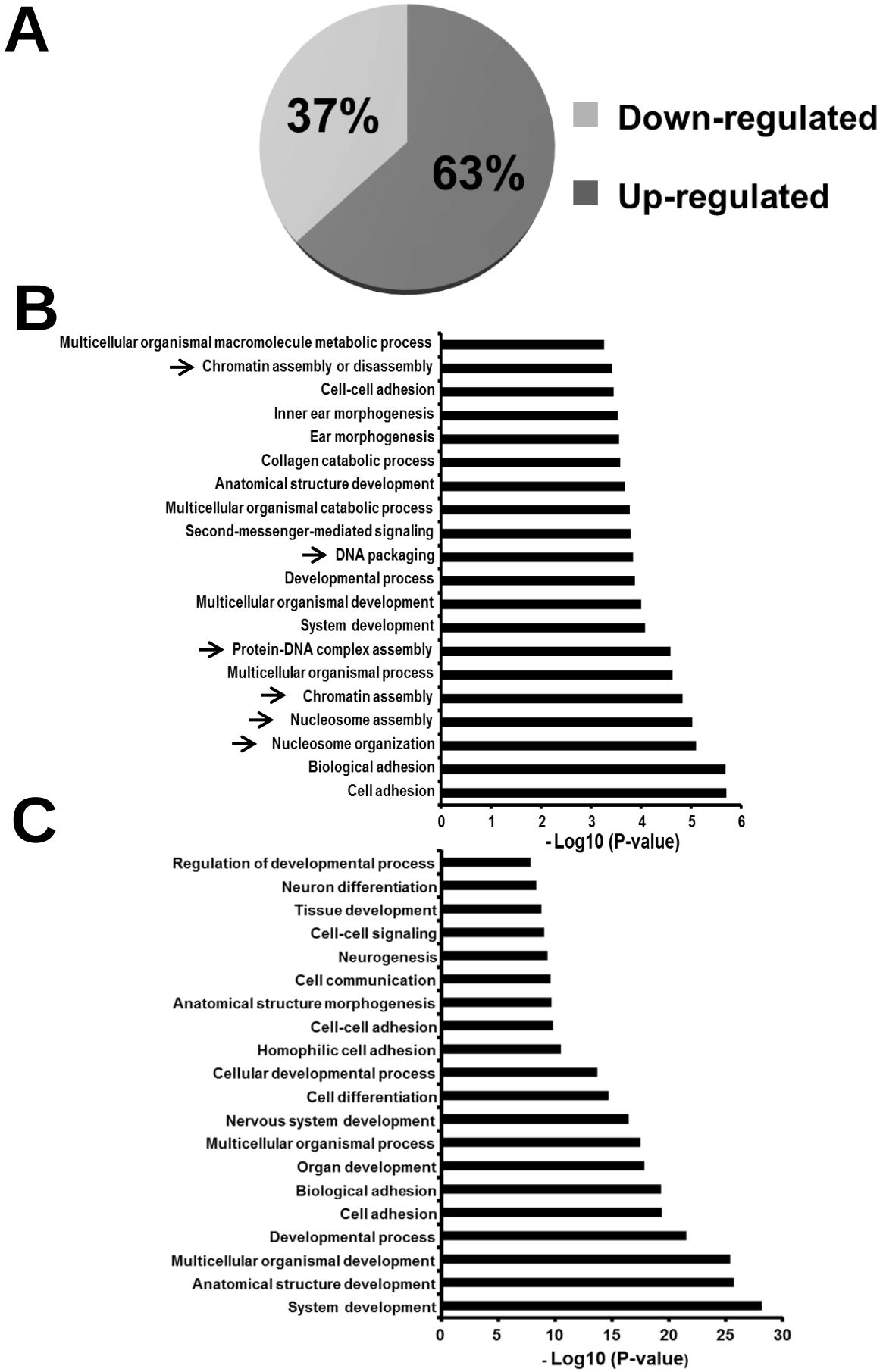
A
37%
63%
Down-regulated
Up-regulated
B
Multicellular organismal macromolecule metabolic process
Chromatin assembly or disassembly
Cell-cell adhesion
Inner ear morphogenesis
Ear morphogenesis
Collagen catabolic process
Anatomical structure development
Multicellular organismal catabolic process
Second-messenger-mediated signaling
DNA packaging
Developmental process
Multicellular organismal development
System development
Protein-DNA complex assembly
Multicellular organismal process
Chromatin assembly
Nucleosome assembly
Nucleosome organization
Biological adhesion
Cell adhesion
0 1 2 3 4 5 6
- Log10 (P-value)
C
Regulation of developmental process
Neuron differentiation
Tissue development
Cell-cell signaling
Neurogenesis
Cell communication
Anatomical structure morphogenesis
Cell-cell adhesion
Homophilic cell adhesion
Cellular developmental process
Cell differentiation
Nervous system development
Multicellular organismal process
Organ development
Biological adhesion
Cell adhesion
Developmental process
Multicellular organismal development
Anatomical structure development
System development
0 5 10 15 20 25 30
- Log10 (P-value)

Figure S4

A

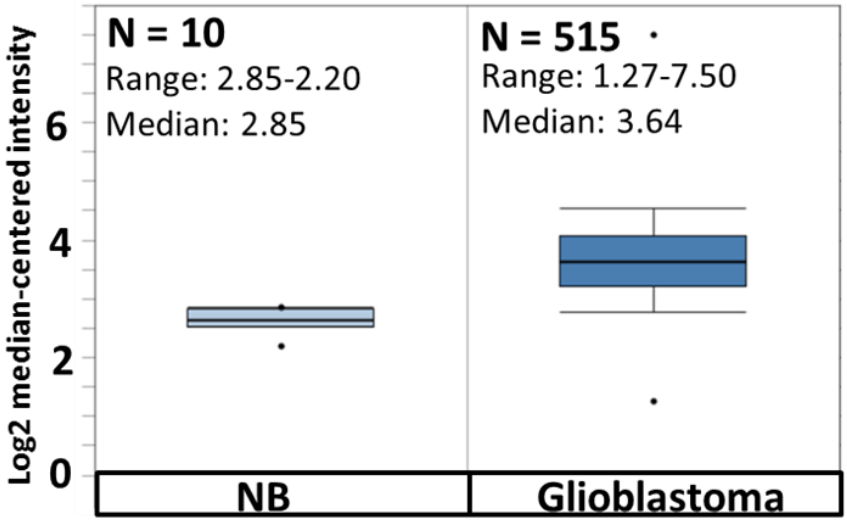

B

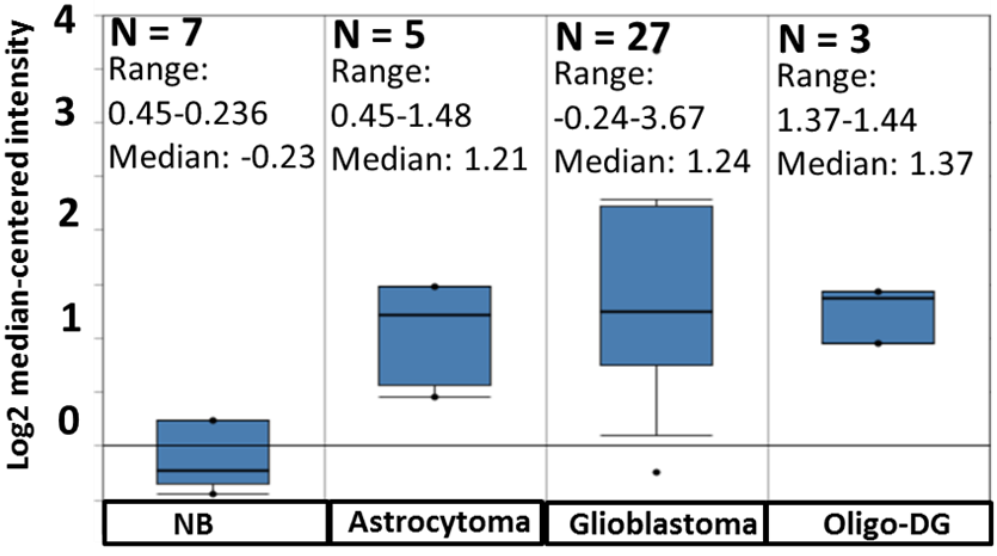

C

MGMT Methylated				MGMT Unmethylated				All			
Standard Estimate				Standard Estimate				Standard Estimate			
	N	Correlation	p-value		N	Correlation	p-value		N	Correlation	p-value
EYA1	61	-0.164	0.207	EYA1	77	0.329	0.0035	EYA1	138	0.129	0.1303
FIGNL1	61	0.356	0.005	FIGNL1	77	0.701	<.0001	FIGNL1	138	0.576	<.0001
MGMT	61	-0.281	0.028	MGMT	77	-0.184	0.1088	MGMT	138	-0.299	0.0004
RAD51	61	0.538	<.0001	RAD51	77	0.575	<.0001	RAD51	138	0.569	<.0001

D

	Overall Survival		
	HR	95% CI	P-value
RBBP4	0.93	0.79-1.09	0.37
RBBP4 Q4	0.77	0.52-1.14	0.19

Cox proportional hazards regression model adjusting for age and MGMT status

HR=Hazard ratio; 95% CI=95% confidence interval

RBBP4 Q4: RBBP4 expression dichotomized as the 4th quartile versus quartiles 1-3

Figure S5

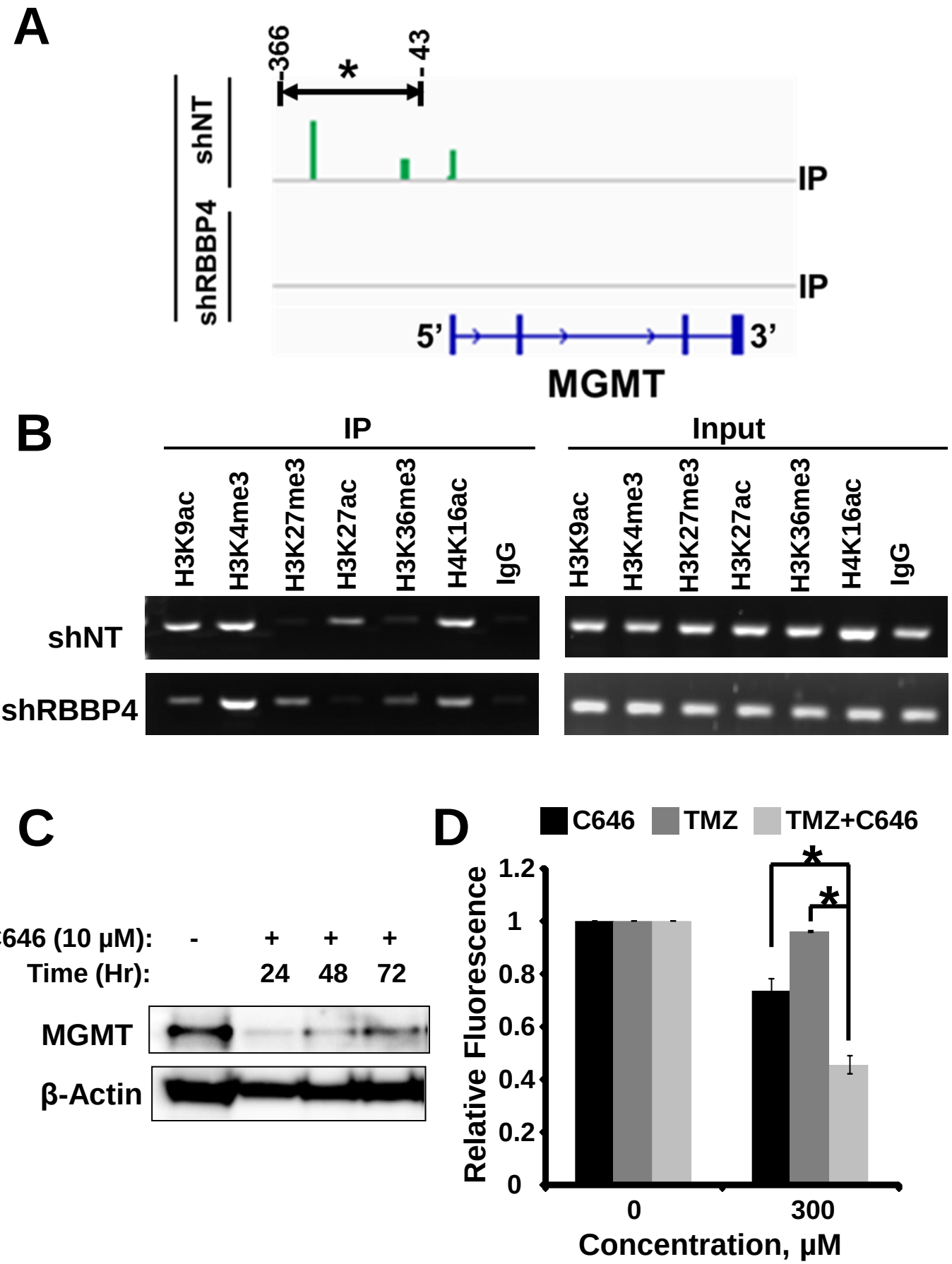
A
-366
-43
*
shNT
shRBBP4
IP
IP
5'
3'
MGMT
B
IP
Input
H3K9ac
H3K4me3
H3K27me3
H3K27ac
H3K36me3
H4K16ac
IgG
shNT
shRBBP4
C
C646 (10 μM): - + + +
Time (Hr): 24 48 72
MGMT
β-Actin
D
C646
TMZ
TMZ+C646
Relative Fluorescence
1.2
1
0.8
0.6
0.4
0.2
0
*
*
0
300
Concentration, μM

Figure S6

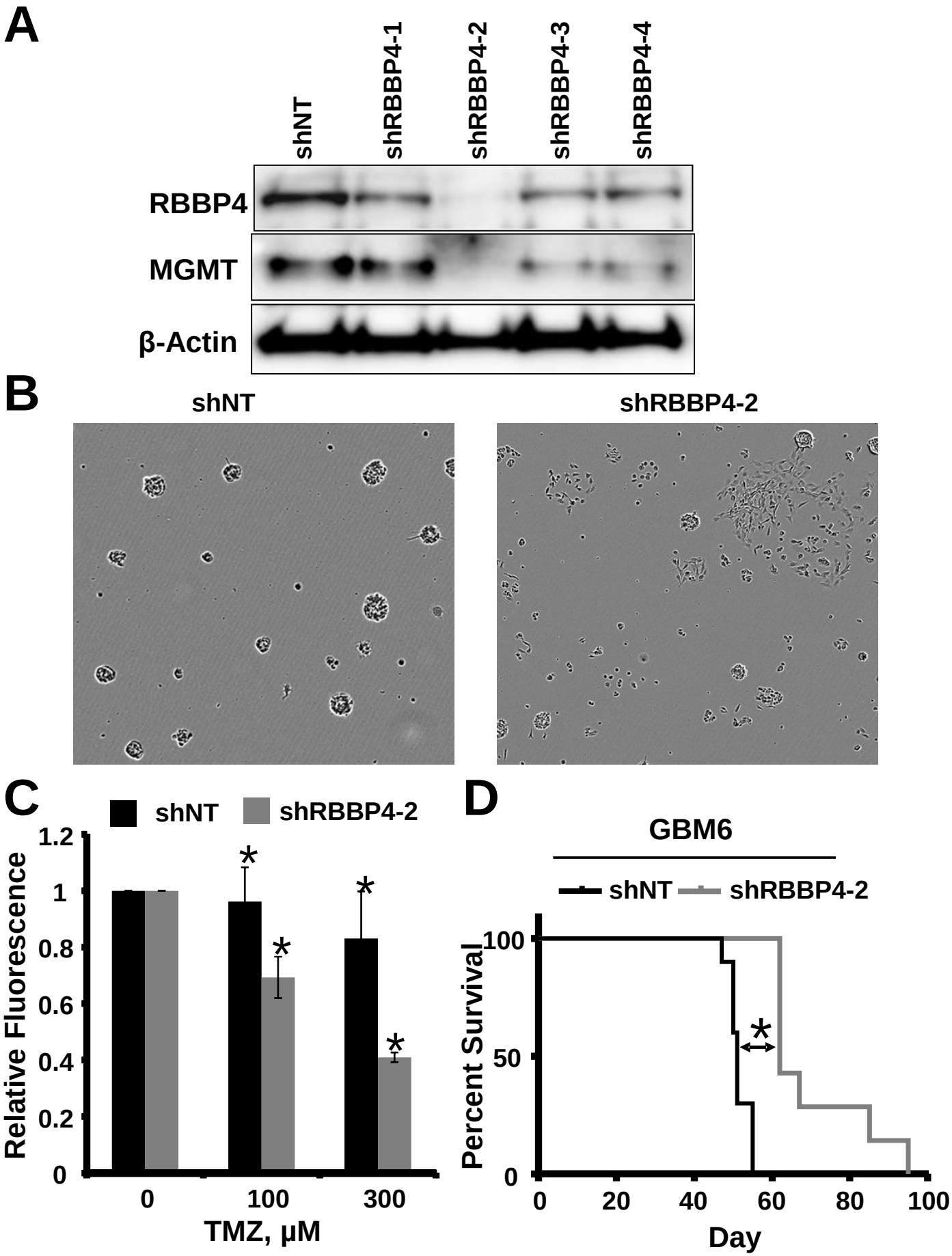
A
shNT
shRBBP4-1
shRBBP4-2
shRBBP4-3
shRBBP4-4
RBBP4
MGMT
β-Actin
B
shNT
shRBBP4-2
C
shNT
shRBBP4-2
Relative Fluorescence
1.2
1
0.8
0.6
0.4
0.2
0
0
100
300
TMZ, μM
*
D
GBM6
shNT
shRBBP4-2
Percent Survival
100
50
0
0
20
40
60
80
100
Day
*

Figure S7

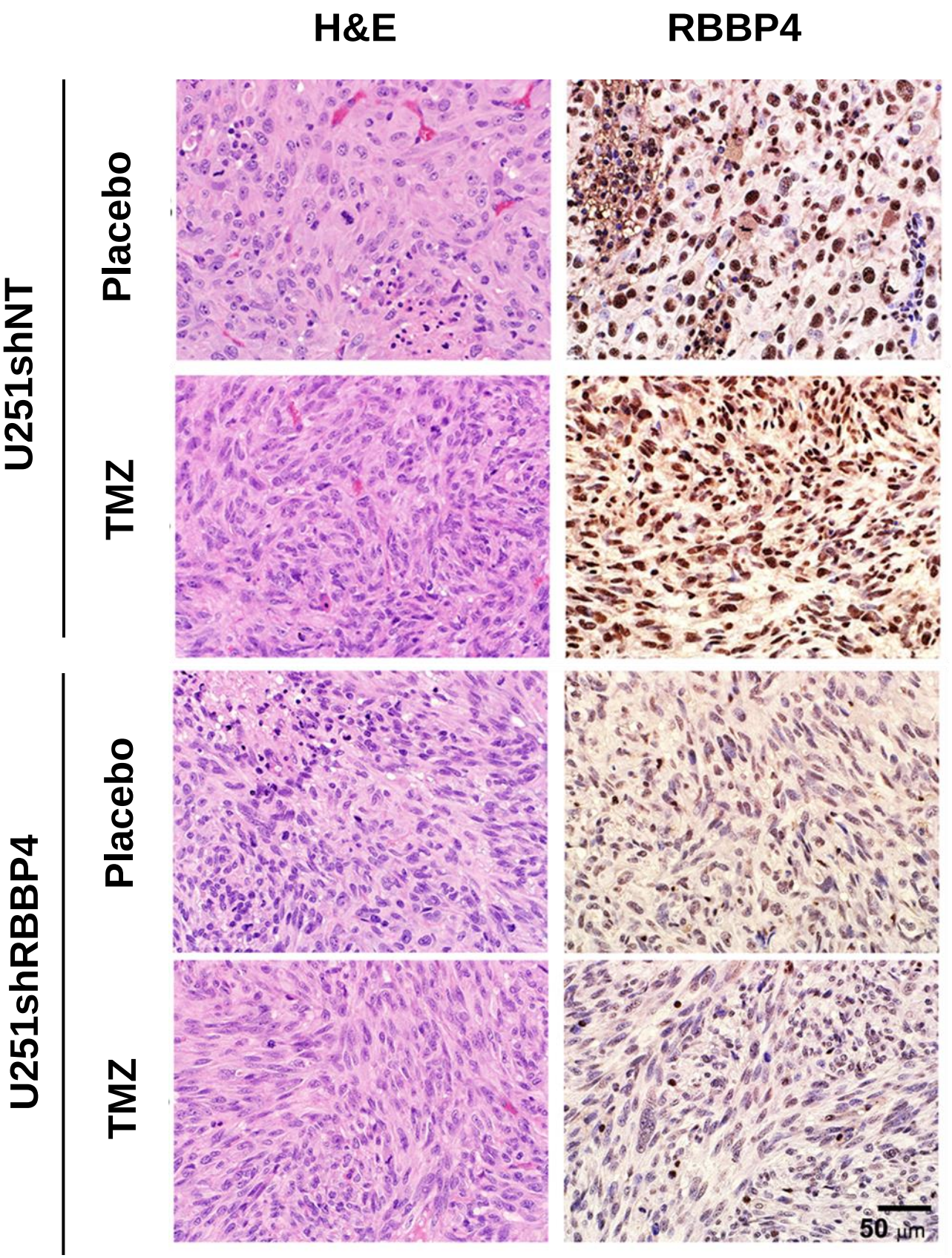
H&E
RBBP4
U251shNT
Placebo
TMZ
U251shRBBP4
Placebo
TMZ
50 µm

Supplemental Figure Legends

Figure S1, related to Figures 2 and 3: Effect of RBBP4 disruption on MGMT expression level and the sensitivity of the indicated anticancer agents. (A) Total RNA extracted from U138 GBM cells expressing the control NT-shRNA or 4 different RBBP4 shRNA constructs was used to evaluated RBBP4 and MGMT expression by real time RT-PCR. (B). Western blot depicting RBBP4 and MGMT levels in U138 GBM cells expressing the control NT-shRNA or 4 different RBBP4 shRNA constructs and β-actin was used as loading control. (C) Sensitivity to DNA alkylating agents TMZ and CCNU (D) sensitivity to ribonuclotide reductase inhibitor hydroxyurea (HU) and DNA crosslinker cisplatin, and (E) sensitivity to radiomimetic bleomycin. * Significant difference ($p<0.05$).

Figure S2, related to Figures 3 and 7: Effect of RBBP4 disruption on RAD51 expression in GBM cells (A-B) RBBP4 and RAD51 expression in U138 and GBM22 cells expressing shNT or shRBBP4. (C) RBBP4 regulates RAD51 in association with H3K9Ac mark within promoter region as evidenced by H3K9Ac ChIPseq comparing T98G-shNT and T98G-shRBBP4cells (D) RNAseq gene read counts in T98G-shNT and T98G-shRBBP4 cells for other key DNA repair genes.

Figure S3, related to Figure 5. Functional distribution of genes regulated by RBBP4 in T98G glioblastoma cells. (A) Number of genes that were suppressed or upregulated following silencing of RBBP4 in T98G GBM cells. (B) The top 20 gene ontologies that were suppressed

following RBBP4 knockdown and (C) Top 20 gene ontologies that were up-regulated following RBBP4 knockdown in T98G cells (arrow = chromatin related ontologies).

Figure S4, related to Figures 3 and 7: Expression of RBBP4 increases with malignancy grade (A) RBBP4 expression in normal brain and GBM according Oncomine TCGA database. (B) RBBP4 expression in gliomas of different malignant grades and histology (NB = normal brain; Oligo-DG = oligodendroglioma) (Oncomine data based on Shai et al., 2003) (C) RBBP4 mRNA expression correlated with MGMT, RAD51, EYA1 and FIGNL1 based on TCGA GBM database. (D) Expression of RBBP4 correlated with overall survival in GBM patients within TCGA database.

Figure S5, related to Figures 4, 5 and 6: Effects of RBBP4 disruption on histone modifications within MGMT promoter region and effect of p300 inhibitor on MGMT expression and TMZ response (A) ChIPseq display of H3K9Ac tags within MGMT promoter region comparing the T98G expressing control shNT and RBBP4 shRNA (* region interrogated by the standard ChIP). (B) ChIP displaying multiple histone marks within MGMT promoter region comparing T98G expressing control shRNA (shNT) with those expressing RBBP4 shRNA (shRBBP4). (C) Western blot showing the effect of p300 inhibitor C646 on MGMT expression. T98G cells were exposed to 10 μM and MGMT expression was evaluated at indicated time-intervals. (D) Bar chart showing p300 inhibitor C646 can sensitize T98G cells to TMZ (Error bars=S.E.M. * significant difference, $p < 0.05$).

Figure S6, related to Figure 7: Effect of RBBP4 disruption on growth and TMZ response in patient-derived xenograft GBM6 (A) Western blot displaying RBBP4 and MGMT expression in GBM6 cells expressing RBBP4 and the control NT shRNAs (B) RBBP4 disruption perturbs neurospheres formation of GBM6 cells (C) RBBP4 disruption sensitizes GBM6 cell In vitro. The bar chart represent data from 3 independent experiments conducted in triplicate (Error bar = S.E.M). (D) Survival of patient derived GBM6 orthotopic xenografts comparing RBBP4 knockdown (shRBBP4-2) with tumors expressing the control shNT. *Significant difference $p<0.05$.

Figure S7, related to Figure 7: Expression of RBBP4 in orthotopic tumors harvested at moribund after completion of TMZ therapy. RBBP4 expression levels in the control U251shNT (upper 2 panels) and RBBP4 knockdown U251shRBBP4 tumors (lower 2 panels). H&E = hematoxylin and Eosin.

Supplemental Tables

Table S1: List of Genes Suppressed by RBBP4 shRNA in T98G Glioblastoma Cells, related to Figure 5.

Table S2: List of Genes Elevated by RBBP4 shRNA in T98G Glioblastoma Cells, related to Figure 5.

Table S3: Ontologies Enriched within Genes Suppressed by RBBP4 shRNA, related to Figure 5

Table S4: Ontologies Enriched within Genes overexpressed by RBBP4 shRNA, related to Figure 5

Supplemental Experimental Procedures

Whole Genome shRNA screening

Primary cells cultured from GBM22 xenograft were used for shRNA screening of genome wide modulators of TMZ response in GBM. GBM22 cells were used in these studies because they do not express MGMT and therefore the mechanisms regulating TMZ sensitivity in this cell line are elusive. Briefly, cells were transduced with a pooled lentiviral shRNA (kindly provided by Dr. Yuichi Machida, Department of Oncology Research, Mayo Clinic in Rochester, MN) at multiplicity of infection (MOI) of approximately 1. This library target about 38,000 genes or 47,000 mRNAs and each shRNA is barcoded with corresponding gene probe sequence used onto U133 plus 2.0 array (Affymetrix, Santa Clara, CA). After a brief selection in puromycin, cells were divided into 2 groups (each in triplicate). One group of the cells was treated with 100 μM TMZ daily for 3 days while the other (control) group received the vehicle DMSO and then allowed to grow for 14 days. Total RNA was extracted from control and cells survived TMZ treatment followed by shRNA amplification according to a protocol supplied by System Biosciences (SBI, Mountain View, CA). The amplified shRNAs were hybridized onto U133 plus 2.0 (Affymetrix) and analysis of shRNA enrichment comparing the control DMSO group with the TMZ treated group was conducted by the Mayo Clinic Bioinformatics core. The shRNAs with higher enrichment in DMSO group but lower enrichment in the TMZ group were considered to represent genes that suppress TMZ sensitivity while those preferentially enriched within the TMZ-treated were considered to enhance TMZ sensitivity.

Cell culture and drug cytotoxicity assay

Briefly, for serum-free primary cultures, flank tumors were mechanically disaggregated and the resulting cell suspensions were plated on laminin-coated flasks in StemPro®NSC-SFM media

(Invitrogen, Carlsbad, CA) supplemented with L- glutamine (Sigma, St. Louis, MO) and 1% penicillin/streptomycin (Invitrogen). After 3-5 days of culture in a humidified incubator at 37°C and 5% CO_2, cells were washed and trypsinized for experiments. The established GBM cell lines T98G and U138 were obtained from American Tissue Culture Collection (ATCC; and plated on tissue culture flasks and cultured in DMEM medium (Invitrogen) supplemented with 10% fetal calf serum (Invitrogen) and 1% penicillin/streptomycin (Invitrogen) in a humidified incubator at 37°C and 5% CO_2. To evaluate cell survival, cells were treated with different concentrations of TMZ or ABT-888 and survival was determined with the CyQuant cell proliferation kit purchased from Life Technologies (Grand Island, NY) or live monitored using IncuCyte ZOOM live cell imaging (Essen BioScience, Ann Arbor, MI).

Antibodies

Rabbit polyclonal antibodies specific for human p300, C-JUN , NF-kB, CBP and SP1 were purchased from Santa Cruz Biotechnology (Santa Cruz, CA) and phospho-KAP1 (S824), total KAP1, phospho-CHK1 (S345), total CHK1, phospho-CHK2 (T68) and total CHK2, H3K9ac and H3K9me3 antibodies were purchased from Cell Signaling Technologies, Inc. (Danvers, MA). Goat polyclonal antibody specific for human RBBP4 (H-19) was purchased from Santa Cruz Biotech, while chromatin immunoprecipitation (ChIP)-grade human anti-RBBP4 (13D10) was from GeneTex (Irvive, CA). Anti-RBBP4 antibody (ab1765; ABCAM, Cambridge, MA) was used for immune-staining. MGMT antibody was purchased from R&D systems, while anti-p-H2AX (Y142) and anti p-H2AX (S139) were from Thermo Fisher Scientific (Waltham, MA). Secondary horseradish conjugated immunoglobulins (IgGs) were obtained from Cell Signaling Technologies, Inc (Danvers, MA) and Thermo Fisher Scientific, respectively.

Phospho-H2AX Foci

T98G cells expressing control shRNA (T98G-shNT) and RBBP4 shRNA ((T98G-shRBBP4) were grown overnight on coverslips. Cells were treated with TMZ or vehicle DMSO and fixed with 4% paraformaldehyde at 0, 24 and 72 hour time points. Irradiated cells (2-Gy) were used as positive control for p-H2AX. The immunofluorescence staining was conducted as described (Gupta et al., 2014). The staining was analyzed with a Leica DMI3000B microscope (North Central Instruments, Plymouth, MN). To quantify foci, at least 200 cells with ≥ 25 foci/nuclei were analyzed for each condition.

RNA- and ChIP-sequencing

Briefly, for RNAseq, total RNA was extracted from cells as described above. The RNA quality was further evaluated using the Agilent 2100 Bioanalyzer (Agilent, Santa Clara, CA). The Illumina TrueSeq RNA Sample preparation Kit v.4.1 (Illumina Inc., San Diego, CA) was used to prepare cDNA libraries from 2 µg of total RNA for RNA-seq, Individual barcoded libraries were analyzed using Agilent 2100 Bioanalyzer (Agilent technologies). Sequencing was carried out on an Illumina HiSeq 2000 machine (Illumina) at Mayo Clinic Medical Genomic Facility. The T98G cells expressing control NT- or RBBP4-shRNA (shRBBP4-3) were used for ChIPseq experiments. Briefly, fixed cells were washed twice with Tris Buffered Saline (TBS) and resuspended in cell lysis buffer (10 mM Tris-HCl, pH7.5, 10 mM NaCl, 0.5% NP-40) and incubated on ice for 10 min. The lysates were washed with MNase digestion buffer (20 mM Tris-HCl, pH7.5, 15 mM NaCl, 60 mM KCl, 1 mM $CaCl_2$) and incubated for 20 minutes at 37 °C in the presence of MNase. After adding the same volume of sonication buffer (100 mM Tris-HCl, pH 8.1, 20 mM EDTA, 200 mM NaCl, 2% Triton X-100, 0.2% sodium deoxycholate), the lysate was sonicated for 15 min (30 sec-on / 30 sec-off) and centrifuged at 15,000 rpm for 10 min. The

cleared supernatant equivalent to 1 – 4 x 10^6 cells was incubated with 2 µg of H3K9Acantibody or normal IgG on a rocker overnight. After adding 30 µl of prewashed protein G-agarose beads, the reactions were further incubated for 3 hours. The beads were extensively washed with ChIP buffer, high salt buffer, $LiCl_2$ buffer, and TE buffer. Bound chromatins were eluted and reverse-crosslinked at 65°C overnight. DNAs were purified using Min-Elute PCR purification kit (Qiagen) after treatment of RNase A and proteinase K. The enrichment was analyzed by targeted real-time PCR in positive and negative genomic loci. For next-generation sequencing, ChIP-seq libraries were prepared from 10 ng of ChIP and input DNAs with the Ovation Ultralow DR Multiplex system (NuGEN, San Carlos, CA). The ChIP-seq libraries were sequenced to 51 base pairs from both ends using the Illumina HiSeq 2000 in the Mayo Clinic Medical Genomics Core. The peaks were identified using SICER or Macs algorithm from BWA-mapped reads.

Animal Studies

All orthotopic animal studies were conducted according to a protocol approved by the Mayo Institutional Animal Care and Use Committee. To evaluate the effect of RBBP4 on TMZ sensitivity U251 expressing RBBP4 shRNA (shRBBP4) or the non-specific targeting control shRNA (shNT) were injected (3 × 10^5 cells per mouse, suspended in 10 µl of PBS) into the right basal ganglia of anesthetized athymic nude mice (Athymic Ncr-nu/nu: Harlan, Indianapolis, IN). Just before treatment initiation, animals were randomized to treatment groups of 10 mice each. Treatment was initiated 2 weeks prior to the time mice were expected to become moribund, as determined from previous studies with each xenograft line. TMZ was purchased from the Mayo Clinic pharmacy and suspended in Ora-plus (Paddock Laboratories, Minneapolis, MN, USA) for oral administration. All doses were administered by oral gavage and a total of 3 cycles (50 mg/kg daily X 5 days repeated after every 28 days) were given. To evaluate whether RBBP4

knockdown alone can impact survival orthotopic GBM6 shRBBP4 (10 mice) and GBM6shNT (10 mice) tumors were monitored without TMZ therapy. Mice were euthanized when they reached a moribund state.

Immunohistochemistry staining

Sections (5 μm) were cut from formalin-fixed paraffin-embedded blocks of tumors harvested after mice died due to intracranial U251 tumors after placebo and TMZ treatment schedules. Sections were deparaffinized in xylene followed by rehydration in graded concentrations of ethanol and finally in water. The antigen retrieval was conducted by boiling sections in sodium citrate (pH. 6.0) in 20 minutes. After cooling down sections were rinsed in water and non-specific peroxidase activity was blocked by 20 min incubation in 0.3% H2O2 in methanol. Primary antibody was diluted to 1:50 and all subsequent steps were performed according to a protocol supplied by the Vectastain Elite ABC Universal kit (Vector Laboratories, Burlingame, CA). Sections were dehydrated in increased concentrations of ethanol and finally in xylene. After mounted with cover slips, sections were air dried and photomicrographs were taken under microscope at 40X magnification.

Real time PCR

Briefly, the real time PCR primers and probes (MGMT, catalogue no. HS00172470_m1 and GAPDH, catalogue no. HS99999905_m1) were purchased from ABI. The SYBR® Green PCR Master Mix was used for RBBP4, RAD51, FIGNL1, EYA1 and β-actin real time PCR using primer sequences listed in the supplemental experimental procedures. Each sample was amplified in triplicate. The relative expression levels were determined using ViiA7 RUO SW V1.1 software (ABI).

List of primers used for qRT-PCR, ChIP and Re-ChIP

qRT-PCR	Forward	Reverse
RBBP4	5'CCCAATGAACCTTGGGTGATTTGTTC3'	5'ACGCTTCCTTCAGGGTCTTCATCA3'
RAD51	5'TGGCCCACAACCCATTT3'	5'GCAACAGCCTCCACAGTAT3'
FIGNL1	5'CTGCTTGTGTTCGATTTCTGATAC3'	5'GCGAAGTAATTCTTCTGCCATTC3'
EYA1	5'GTCAGGAATGGAGGTTTGCTA3'	5'-CTGAACTGGCTTGAGATGTTTG-3'
β-Actin	5'CCAGAGATGGCCACGGCTGCT3'	5'TCCTTCTGGATCCTGTCGGGA3'
ChIP-ReChIP		
RBBP4	5'GCCCCGGATATGCTGGGAC3'	5'GGGCAACACCTGGGAGGCAC3'
RAD51	5′CCCCCGGCATAAAGTTTGA3′	5′GCTTTCAGAATTCCCGCCA3
MGMT	5′ GACAGGAAAAGGTACGGGCCATT 3′	5′GAGCCGAGGACCTGAGAAAAGCAAG 3′

Identity and sequences of shRNA used to target human RBBP4

Name	Open Biosystems OligoID	Sequences
RBBP4-1	V2LHS_247612	TGCTGTTGACAGTGAGCGCGGCTAGAGTGAGTAAGGAATATAGTGAAGCCACAGATGTATATTCCTTACTCACTCTAGCCTTGCCTACTGCCTCGGA
RBBP4-2	V2LHS_57087	TGCTGTTGACAGTGAGCGAGCCACCAGAGTTGTTGTTTATTAGTGAAGCCACAGATGTAATAAACAACAACTCTGGTGGCCTGCCTACTGCCTCGGA
RBBP4-3	V2LHS_57090	TGCTGTTGACAGTGAGCGCAGCCACAGACTTAACGTTGAATAGTGAAGCCACAGATGTATTCAACGTTAAGTCTGTGGCTTTGCCTACTGCCTCGGA
RBBP4-4	V2LHS_57091	TGCTGTTGACAGTGAGCGCGGGTCCTAGATATGTCTTTACTAGTGAAGCCACAGATGTAGTAAAGACATATCTAGGACCCTTGCCTACTGCCTCGGA

Statistical Analysis

The RNA-Seq data was analyzed using MAP-RSeq v.1.2.1 (Kalari et al., 2014), the Mayo Bioinformatics Core pipeline. MAP-RSeq consists of alignment with TopHat 2.0.6 (Kim et al.,

2013) against the hg19 genome build and gene counts with the HTSeq software 0.5.3p9 (http://www.huber.embl.de/users/anders/HTSeq/doc/overview.html) using gene annotation files obtained from Illumina (http://cufflinks.cbcb.umd.edu/igenomes.html). Expression for each gene was normalized by correcting for gene length and reported as RPKM (Reads Per Kilobase per Million mapped reads) values. ChIPseq data were analyzed using the HiChIP pipeline (Yan et al., 2014). In brief, the 51-bp paired-end reads were aligned to the human reference sequence hg19 using BWA (version 0.5.9). Only mapped pairs with one or both ends aligning to unique locations were retained and duplicates were further filtered out using Picard Mark Duplicates command. Peaks were identified using the MACS package (version 2.0.10) at the cutoff of q value <=0.01 and fold change >=2 over the IgG control. The ngs.plot package (Shen et al., 2014) was used to generate heatmap for genes showing differential expression between T98G-shNT and T98G-shRBBP4, which illustrated the H3K9Ac binding profile (number of reads per million) from upstream 4kb to downstream 4kb of selected genes. In the plots, genes were sorted in descending order based on expression level.

Supplemental References

Gupta, S.K., Carlson, B.L., Boakye-Agyeman, F., Bakken, K.K., Kizilbash, S.H., Schroeder, M.A., Reid, J, Sarkaria, J.N. (2014) Discordant in vitro and in vivo chemopotentiating effects of the PARP inhibitor veliparib in temozolomide-sensitive versus -resistant glioblastoma multiforme xenografts. Clin Cancer Res 20, 3730-3741

Kalari, K. R., Nair, A. A., Bhavsar, J. D., O'Brien, D. R., Davila, J. I., Bockol, M. A., Nie, J., Tang, X., Baheti, S., Doughty, J. B., et al. (2014). MAP-RSeq: Mayo Analysis Pipeline for RNA sequencing. BMC Bioinformatics 15, 224.

Kim, D., Pertea, G., Trapnell, C., Pimentel, H., Kelley, R., and Salzberg, S. L. (2013). TopHat2: accurate alignment of transcriptomes in the presence of insertions, deletions and gene fusions. Genome Biol 14, R36.

Shai R, Shi T, Kremen TJ, Horvath S, Liau LM, Cloughesy TF, Mischel PS, Nelson SF (2003).

Gene expression profiling identifies molecular subtypes of gliomas. Oncogene 31, 4918-4923

Yan, H., Evans, J., Kalmbach, M., Moore, R., Middha, S., Luban, S., Wang, L., Bhagwate, A., Li, Y., Sun, Z., et al. (2014). HiChIP: a high-throughput pipeline for integrative analysis of ChIP-Seq data. BMC Bioinformatics 15, 280.